# Spin-dependent forces and electromagnetic structure of the nucleon

X. Song and J. S. McCarthy
*Institute of Nuclear and Particle Physics and Department of Physics, University of Virginia, Charlottesville, Virginia 22901*

(Received 18 May 1992)

The spin-dependent forces, which can arise from either nonperturbative instanton effects or perturbative color magnetic interactions, cause the difference between $u$-quark and $d$-quark spatial distributions inside the nucleon. Considering this SU(6) symmetry-breaking effect, the elastic electromagnetic nucleon form factors and static magnetic moments of octet baryons can be well reproduced in the center-of-mass (c.m.) bag model. The same spin force effects on the deep inelastic polarized structure functions are also discussed.

PACS number(s): 24.85.+p, 13.40.Fn, 13.60.Hb

## I. INTRODUCTION

It has been shown that color magnetic spin-spin interactions play a very important role in explaining hadron mass spectroscopy [1,2], the magnetic moments of baryons [3,4], and the nonzero neutron electric form factor [5]. The electric form factor of the neutron would be zero if the nucleon wave function were exactly SU(6) symmetric. It was shown [5] that the SU(6) violation, arising from configuration mixing in the nucleon due to the color hyperfine interactions, gives a rather good agreement with experiment for the neutron charge radius and form factor.

However, color magnetic spin force, which is based on perturbative quantum chromodynamics (QCD) and derived from one-gluon exchange Breit-Fermi interactions, might not be a unique source of SU(6) symmetry breaking and is questionable at low energies. Another possible and, perhaps, more important spin-dependent force comes from nonperturbative instanton-induced interactions [6–8]. The spin force generated by instanton effects has the same form $\boldsymbol{\sigma}_i\cdot\boldsymbol{\sigma}_j\delta(\mathbf{r}_i-\mathbf{r}_j)$ as the color magnetic interactions and has been used to successfully explain the hadron spectroscopy [9–11]. In this approach, the scalar diquark, for instance, the $u$-$d$ quark pair in the neutron, has lighter mass and hence smaller spatial size than the vector diquark due to the instanton interactions. One possible configuration of quark distributions due to this effect is that the two $d$ quarks in the neutron are distributed in the outer region while the $u$ quark is distributed in the inner region. This is very similar to the repulsive vector diquark ($d$-$d$ quark pair in the neutron) configuration given by the color magnetic interaction [5]. In this paper we will show that the spin-dependent effects, which are generated by instantons or color magnetic interactions or both, provide a good description of magnetic moments and electromagnetic form factors of the nucleon and other baryons.

In the deep inelastic region, if the nucleon wave function had exact SU(6) symmetry, $g_1^n(x,Q^2)$ would be zero. The European Muon Collaboration (EMC) data [12] combined with the Bjorken sum rule [13], however, indicate $g_1^n<0$. In this paper we will show that the c.m. bag model with spin-dependent force effects, which give a nonzero $G_E^n(Q^2)$, can lead naturally to a nonzero and negative $g_1^n(x,Q^2)$. The calculated $g_1^p(x,Q^2)$ and its first moment are also compatible with the EMC result.

## II. ELASTIC FORM FACTORS AND MAGNETIC MOMENTS

The electromagnetic form factors are defined by

$$\langle p'|J_\mu(0)|p\rangle=\frac{1}{(2\pi)^3}\left[\frac{M^2}{E_pE_p'}\right]^{1/2}\bar{u}_{s'}(p')\times\left[F_1(Q^2)\gamma_\mu+F_2(Q^2)\frac{i\sigma_{\mu\nu}}{2M}q^\nu\right]u_s(p)\ . \tag{1}$$

In the c.m. bag model [14] the $\gamma NN$ vertex can be written

$$\int d^4y\, e^{iq\cdot y}\langle p'|J_\mu(y)|p\rangle=(2\pi)^4\delta^4(p+q-p')\langle p'|J_\mu(0)|p\rangle$$
$$=(2\pi)\delta^4(p+q-p')\sum_{1\to 2,3}\int\prod_{i=1}^{3}d^4r_i e^{i\mathbf{q}\cdot\mathbf{r}_1}\cdot q^\dagger_{p',\alpha'}(\mathbf{r}_1,\mathbf{r}_2,\mathbf{r}_3)[\hat{e}_q\gamma_0\gamma_\mu]_1 q_{p,\alpha}(\mathbf{r}_1,\mathbf{r}_2,\mathbf{r}_3)\ , \tag{2}$$

 

where

$$q_{p,\alpha}(\mathbf{r}_1,\mathbf{r}_2,\mathbf{r}_3)=q_p(\mathbf{r}_1)q_p(\mathbf{r}_2)q_p(\mathbf{r}_3)\alpha_N \; . \tag{3}$$

$\alpha_N$ is the SU(6) spin-flavor wave function of the nucleon and $q_p(\mathbf{r})$ is the Lorentz-boosted quark wave function [15]:

$$q_p(\mathbf{r})=S(\Lambda)q(\Lambda^{-1}\mathbf{r}) \; , \\ S(\Lambda)-ch\frac{\Omega}{2}+\hat{\mathbf{p}}\cdot\alpha sh\frac{\Omega}{2} \; , \tag{4}$$

where $ch\Omega=E_p/M$ and $q(\mathbf{r})$ is the quark wave function in the nucleon rest frame:

$$q(\mathbf{r})=\frac{1}{N(\omega)^{1/2}}\begin{pmatrix} ij_0\left(\omega\frac{r}{R}\right)U_m \\ -ij_1\left(\omega\frac{r}{R}\right)\sigma\cdot\hat{\mathbf{r}}U_m \end{pmatrix} \; , \tag{5}$$

where $\omega\simeq 2.04$, $\hat{\mathbf{r}}=r/|\mathbf{r}|$, $R$ is the bag radius which can be taken as a parameter in the model, $j_0, j_1$ are spherical Bessel functions, $U_m$ is a two-component Pauli spinor, and $U_{+1/2}=\binom{1}{0}$, $U_{-1/2}=\binom{0}{1}$. The normalization factor is $N(\omega)=\{4\pi R^3[1-j_0^2(\omega)]\}/\omega^2$. By including the spin force effect, the quarks have different spatial wave functions in Eq. (3), the electric form factors of the nucleon in the Breit frame can be written

$$G_E^p(Q^2)=\frac{1}{3}\frac{C}{1+\tau}\int_0^1 x^2dx\left[4j_0\left(\frac{QRx}{\sqrt{1+\tau}}\right)-j_0\left(\frac{QR\xi x}{\sqrt{1+\tau}}\right)\right][j_0^2(\omega x)+j_1^2(\omega x)] \tag{6}$$

and

$$G_E^n(Q^2)=-\frac{2}{3}\frac{C}{1+\tau}\int_0^1 x^2dx\left[j_0\left(\frac{QRx}{\sqrt{1+\tau}}\right)-j_0\left(\frac{QR\xi x}{\sqrt{1+\tau}}\right)\right][j_0^2(\omega x)+j_1^2(\omega x)] \; , \tag{7}$$

where $C=\omega^2/[1-j_0^2(\omega)]$ is a positive constant, $R$ denotes the radius of the $u$-quark spatial distribution in the proton ($R_u^p$), or the radius of $d$-quark distribution in the neutron ($R_d^n$) and $\tau=Q^2/4M^2$. The symmetry-breaking parameter $\xi$ denotes the ratio between the radius of $d$-quark distribution and $u$-quark distribution in the proton: $\xi=R_d^p/R_u^p=R_u^n/R_d^n$, where isospin symmetry is assumed, i.e., the $u(d)$-quark distribution in the neutron is the same as the $d(u)$-quark distribution in the proton. In Eq. (7) the first term $j_0(QRx/\sqrt{1+\tau})$ comes from the struck $d$ quark (in the neutron) and the second term $j_0(QR\xi x/\sqrt{1+\tau})$ is struck $u$-quark contribution. Several observations are as follows.

(i) The $1+\tau$ and $\sqrt{1+\tau}$ factor in (6) and (7) comes from a Lorentz boost of the quark wave functions, hence relativistic effects have been taken into account.

(ii) In the SU(6) symmetry limit of $\xi=1$, Eq. (7) gives $G_E^n(Q^2)=0$ while Eq. (6) reduces into the result of Ref. [15]. The spin-dependent interactions break the SU(6) symmetry and lead to $R_u^n<R_d^n$ and $\xi<1$, this gives a nonzero $G_E^n(Q^2)$ as shown in Fig. 1.

(iii) It should be noted that for the neutron electric form factor the coefficient $(-\frac{2}{3})$ in Eq. (7) comes from the matrix element of the struck quark charge operator $\hat{e}_q$ and is negative. On the other hand, the $u$-quark contribution in the second term of Eq. (7), is larger than the $d$-quark contribution in the first term, so that the neutron charge form factor and its slope at $Q^2=0$ are both positive.

(iv) The parameter $\xi$ can be determined by fitting the rms charge radius of the proton. From (6) and $\langle r_p^2\rangle_{\rm exp}=0.682$ fm$^2$, we obtain $\xi\simeq 0.83$. Using this value we predict the neutron charge radius $\langle r_n^2\rangle=-0.112$ fm$^2$, which agrees very well with data [16]: $\langle r_n^2\rangle_{\rm exp}=-0.117$ fm$^2$. It is interesting to note that from (6) and (7) we have

$$\frac{\langle r_n^2\rangle}{\langle r_p^2\rangle-\frac{3}{2M^2}}=-\frac{2(1-\xi^2)}{4-\xi^2} \; . \tag{8}$$

With $\xi=0.83$, rhs$=-0.188$, while using the data one ob-

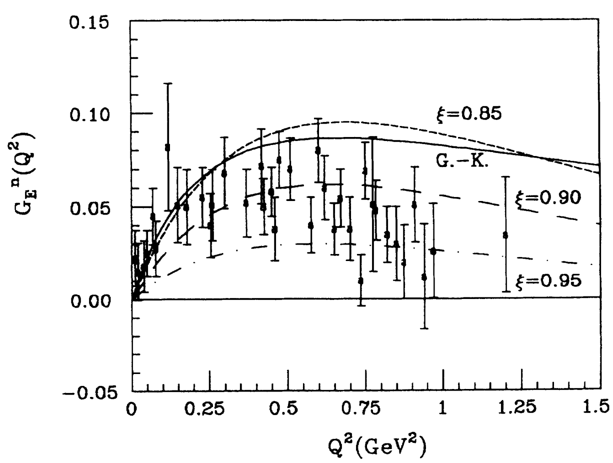


FIG. 1. Comparison of the $G_E^n(Q^2)$ calculated in the symmetry-breaking c.m. bag model with the data. Solid curve is phenomenological fit given by Gari and Krumpelmann [16].

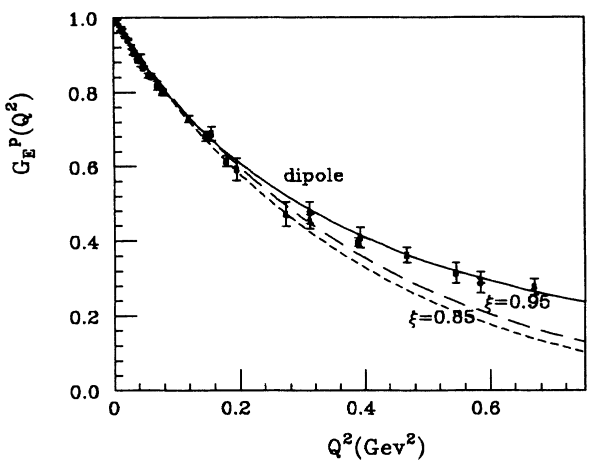


FIG. 2. Comparison of the calculated $G_E^p(Q^2)$ with the data.

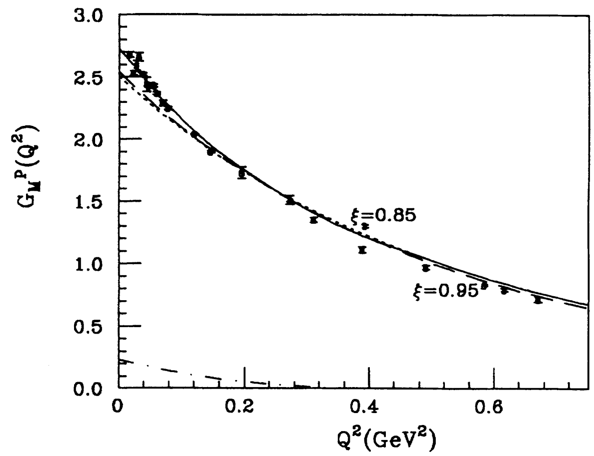


FIG. 4. Comparison of the calculated $G_M^p(Q^2)$ with the data. The notation of lines is the same as in Fig. 3.

tains lhs$=-0.190$. The agreement is excellent.

(v) The result for $G_E^p(Q^2)$ is shown in Fig. 2 and the agreement with data is quite good. One can see that the proton electric form factor is not as sensitive to the spin-dependent effects as in the neutron case. This is because the $u$-quark contributions, $4j_0(QRx/\sqrt{1+\tau})$ term in (6), dominate the integral. The situation for the neutron is quite different; for SU(6) symmetric wave function the $u$-quark and $d$-quark contributions cancel each other in (7) and lead to $G_E^n(Q^2)=0$, so a nonzero neutron charge form factor is very sensitive to the symmetry-breaking effects or the parameter $\xi$.

(vi) Similarly, one can obtain the magnetic form factors of the nucleon, $G_M^p(Q^2)$ and $G_M^n(Q^2)$. The numerical results are shown in Figs. 3 and 4. The theoretical predictions agree well with the experimental data except for $Q^2<0.3$ GeV$^2$. However, in the low-$Q^2$ region pion cloud corrections should be added (e.g., see Ref. [17]).

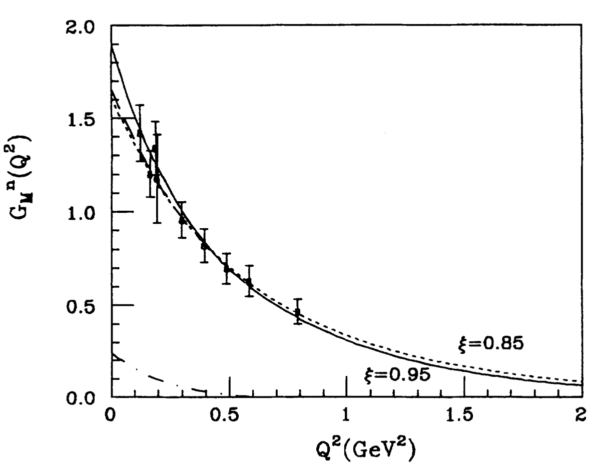


FIG. 3. Comparison of the calculated $G_M^n(Q^2)$ with the data. Long dash curve: $\xi=0.95$; short dash curve: $\xi=0.85$; dot-dashed curve: pion cloud correction; solid curve: $\xi=0.85$ plus pion cloud correction.

For the static magnetic moments we obtain

$$\frac{\mu_n}{\mu_p}=-\frac{2}{3}(1-\epsilon)\ , \quad \epsilon=\frac{8MR(1-\xi)}{4MR(8+\xi)+27I_1/I_0}\ , \tag{9}$$

where

$$\begin{aligned} I_0&=\int_0^1 x^3 dx j_0(\omega x) j_1(\omega x)\ , \\ I_1&=\int_0^1 x^2 dx [j_0^2(\omega x)-\tfrac{1}{3}j_1^2(\omega x)]\ . \end{aligned} \tag{10}$$

Hence we have $\mu_n/\mu_p=-0.65$ which is compatible with the data: $(\mu_n/\mu_p)_{\exp}=-0.68$. The small discrepancy could be removed by including the pion cloud corrections. In the SU(6) symmetry limit, $\xi\to 1, \epsilon\to 0$, from (9), the well-known SU(6) result $\mu_n/\mu_p=-\frac{2}{3}$ is reproduced.

(vii) To verify whether the same spin-dependent force effect also provides a good description of electromagnetic structure of the hyperons, we examine the $\Sigma^+$ hyperon which has the same SU(6) wave function as the proton but with an $s$ quark replacing the $d$ quark. We assume the $u$-quark spatial distributions in $\Sigma^+$ are the same as that in the proton, while the $s$-quark distribution in $\Sigma^+$ is closer to the center than the $d$ quark in the proton because, in addition to the spin force effect, there is a quark mass effect ($m_s>m_d$). Using $\xi_s$ to denote the ratio between the radius of the $s$-quark distribution and that of the $u$-quark distribution in $\Sigma^+$, we should have $\xi_s\le\xi\le 1$. From the data $\mu_{\Sigma^+}=2.42$ nm we obtain $\xi_s\simeq 0.70$. Using the symmetry-breaking parameters $\xi=0.85$ and $\xi_s=0.70$ ($R=1.0$ fm), we calculate the magnetic moments of octet baryons. The comparisons of our results with data and other models [17–21] are listed in Table I. The agreement is quite good. It should be noted that for the $\Lambda$ hyperon, there are no pion cloud corrections hence less ambiguities. Our result $\mu_\Lambda=-0.616$ nm agrees very well with the data ($-0.613\pm0.004$).

TABLE I. Comparison of the calculated magnetic moments of baryons with data and other models.

| Baryon | Data | This paper | NQM[a] | SKM[b] | BSM[c] | CQM[d] |
|---|---|---|---|---|---|---|
| $p$ | 2.793 | 2.736 | 2.70 | 2.03 | 1.87 | 2.696 |
| $n$ | $-1.913$ | $-1.971$ | $-1.80$ | $-1.58$ | $-1.31$ | $-1.991$ |
| $\Lambda$ | $-0.613\pm0.004$ | $-0.616$ | $-0.59$ | $-0.71$ | $-0.41$ | $-0.614$ |
| $\Sigma^+$ | $2.42\pm0.05$ | 2.423 | 2.59 | 1.99 | 2.07 | 2.475 |
| $\Sigma^0$ | | 0.728 | 0.81 | 0.60 | 0.51 | |
| $\Sigma^-$ | $-1.157\pm0.025$ | $-1.070$ | $-1.01$ | $-0.79$ | $-1.05$ | $-1.088$ |
| $\Xi^0$ | $-1.25\pm0.014$ | $-1.309$ | $-1.36$ | $-1.55$ | $-1.15$ | $-1.365$ |
| $\Xi^-$ | $-0.679\pm0.031$ | $-0.650$ | $-0.46$ | $-0.64$ | $-0.14$ | $-0.552$ |

[a]References [18 and 19].
[b]Reference [20].
[c]Reference [21].
[d]Reference [17].

## III. DEEP INELASTIC STRUCTURE FUNCTIONS

A detailed discussion of the deep inelastic structure functions of the nucleon in the c.m. bag model with spin force effects will be given elsewhere. Here we only list part of the result and give a brief discussion on spin-dependent structure function $g_1$. In the MIT bag model [22], where as a result of SU(6) symmetry, $g_1^n(x)=0$. However, including the symmetry-breaking effects, $g_1^n(x)$ would be nonzero. The result from the c.m. bag model is shown in Fig. 5. The corresponding $g_1^p(x)$ is shown in Fig. 6. Several comments are in order.

(i) The structure function $g_1^n(x)$ is nonzero and negative. This is because the structure function comes from the hadronic tensor and is proportional to the matrix element of axial vector current: $\langle N|\hat{e}_q^2\gamma_\mu\gamma_5|N\rangle$. Using the bag-model quark wave function, this matrix element can be reduced into a product of the matrix element $U_m^\dagger\hat{e}_q^2\sigma_z U_m$ and the integral involving the quark spatial wave function, where $\hat{e}_q^2$, $\sigma_z$, and $U_m$ are the squared charge operator, spin projection operator, and the Pauli spinor of the struck quark. We note that, contrary to the elastic electric form factor in Eq. (7) (where only the struck quark charge operator is involved and the coefficient is negative) the coefficient before the spatial integral now becomes positive. Due to the spin force effects the $u$-quark spatial integral has more weight than $d$ quark, so that $g_1^n$ becomes negative.

(ii) Similar to the neutron electric form factor, $g_1^n$ is very sensitive to the symmetry-breaking effects (or $\xi$). Measurements of $g_1^n$ with high accuracy would thus be quite helpful in understanding nucleon structure.

(iii) The symmetry-breaking effects reduce $g_1^p(x)$ and its first moment as shown in Fig. 6. The numerical result shows that $\int_0^1 dx\, g_1^p(x)=0.109$ for $\xi=0.85$, which is compatible with the EMC data $(0.126\pm0.010\pm0.015)$.

(iv) Since $\int_0^1 dx\, g_1^n(x)\simeq-0.03$, hence $\int_0^1 dx\,[g_1^p(x)-g_1^n(x)]\simeq0.14$, which is less than that expected from the Bjorken sum rule ($g_A/6$, even we use c.m. bag-model value $g_A=0.109$). However, the small-$x$ behavior of $g_1^p$ and $g_1^n$ is not clear and depends on different assumptions [23,24]. As we discussed in the unpolarized case [14], in the small-$x$ region ($x<0.3$) the Regge corrections and sea quark contributions should not be ignored. In the Bjorken sum rule, the polarized sea quark contributions in $g_1^p$ and $g_1^n$ cancel, but the Regge contributions do not. Hence a suitable Regge term could increase the $g_1^p$ and reduce $g_1^n$, and the Bjorken sum rule might be restored.

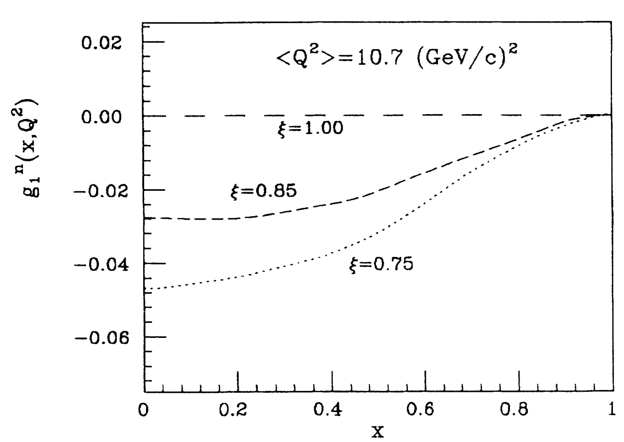


FIG. 5. Calculated $g_1^n(x)$ from symmetry-breaking c.m. bag model.

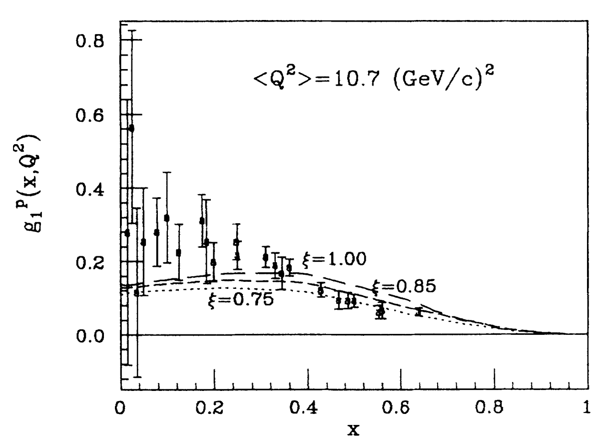


FIG. 6. Comparison of the calculated $g_1^p(x)$ with the EMC data at $\langle Q^2\rangle=10.7(\mathrm{GeV}/c)^2$.

## IV. SUMMARY

We have shown that the c.m. bag model with the spin-dependent forces, which are generated by nonperturbative instanton interactions or perturbative color magnetic interactions or both, provides a satisfactory description of the static magnetic moments and elastic form factors of the nucleon and other baryons (with small pion cloud corrections at very low-$Q^2$ region), and can also qualitatively describe the deep inelastic nucleon structure functions except for small-$x$ region, where the Regge and sea quark contributions should be included.

## ACKNOWLEDGMENTS

The authors would like to thank H. J. Weber for many stimulating discussions. The authors also thank P. K. Kabir, R. Lourie, and O. Rondon-Aramayo for their comments and suggestions. This work was supported by the U.S. Department of Energy and the Commonwealth Center for Nuclear and High Energy Physics, Virginia.

[1] A. De Rújula, H. Georgi, and S. L. Glashow, Phys. Rev. D **12**, 147 (1975).
[2] N. Isgur and G. Karl, Phys. Rev. D **18**, 4187 (1987); **20**, 2653 (1979).
[3] N. Isgur and G. Karl, Phys. Rev. D **21**, 3175 (1980).
[4] H. J. Lipkin, in *Intersections Between Particle and Nuclear Physics,* Steamboat Springs, Colorado, Proceedings of the Conference, edited by Richard E. Mische, AIP Conf. Proc. No. 123 (AIP, New York, 1984), p. 346.
[5] N. Isgur, G. Karl, and D. W. L. Sprung, Phys. Rev. D **23**, 163 (1981).
[6] A. A. Belavin *et al.*, Phys. Lett. **59B**, 85 (1975).
[7] G. 't Hooft, Phys. Rev. D **14**, 3432 (1976).
[8] E. V. Schuryak, Nucl. Phys. **B214**, 237 (1983).
[9] E. V. Schuryak and J. L. Rosner, Phys. Lett. B **218**, 72 (1989).
[10] J. Dey, M. Dey, and P. Volkovitsky, Phys. Lett. B **261**, 493 (1991).
[11] W. H. Blask *et al.*, Z. Phys. A **337**, 327 (1990).
[12] J. Ashman *et al.*, EMC Collaboration, Nucl. Phys. **B328**, 1 (1989).
[13] J. D. Bjorken, Phys. Rev. **148**, 1467 (1966); Phys. Rev. D **1**, 1376 (1970).
[14] X. M. Wang, X. Song, and P. C. Yin, Hadron J. **6**, 985 (1983).
[15] X. M. Wang and P. C. Yin, Phys. Lett. **140B**, 249 (1984).
[16] M. Gari and W. Krumpelmann, Z. Phys. A **322**, 689 (1985).
[17] J. Cohen and H. J. Weber, Phys. Lett. **165B**, 229 (1985).
[18] D. B. Lichtenberg, Phys. Rev. D **15**, 345 (1977).
[19] J. Franklin, Phys. Rev. D **30**, 1542 (1984).
[20] N. W. Park, J. Schechter, and H. Weigel, Phys. Rev. D **43**, 869 (1991).
[21] J. Kunz and P. J. Mulders, Phys. Lett. B **231**, 335 (1989).
[22] R. J. Hughes, Phys. Rev. D **16**, 622 (1977).
[23] F. E. Close and R. G. Roberts, Phys. Rev. Lett. **60**, 1471 (1988).
[24] X. Song and J. Du, Phys. Rev. D **40**, 2177 (1989).